A&A 551, A31 (2013)
DOI: 10.1051/0004-6361/201219433

Astronomy & Astrophysics

An MK-like system of spectral classification for hot subdwarfs⋆

J. S. Drilling[1], C. S. Jeffery[2], U. Heber[3], S. Moehler[4], and R. Napiwotzki[5]

[1] Department of Physics and Astronomy, Louisiana State University, Baton Rouge, LA 70803, USA
e-mail: johndrilling@comcast.net
[2] Armagh Observatory, College Hill, Armagh BT61 9DG, Northern Ireland
e-mail: csj@arm.ac.uk
[3] Dr. Remeis Sternwarte, Universität Erlangen-Nürnberg, 96049 Bamberg, Germany
e-mail: Ulrich.Heber@sternwarte.uni-erlangen.de
[4] European Southern Observatory, Karl-Schwarzschild-Strasse 2, 85748 Garching, Germany
e-mail: smoehler@eso.org
[5] Centre for Astrophysics Research, University of Hertfordshire, College Lane, Hatfield AL10 9AB, UK
e-mail: r.napiwotzki@gmail.com

Received 17 April 2012 / Accepted 27 November 2012

ABSTRACT

An MK (Morgan-Keenan)-like system of spectral classification for hot subdwarfs is presented. We find that a three-dimensional spectral type, consisting of a "spectral" class, a "luminosity" class, and a "helium" class, is necessary to classify the sdO (subdwarf O) and sdB (subdwarf B) stars. In addition, the helium-strong stars appear to form two parallel spectral sequences: one showing strong lines of CII, CIII, or CIV, and the other with these same lines weak or absent. We also give a preliminary calibration of the new spectral types in terms of effective temperature, surface gravity, and surface helium-to-hydrogen abundance ratio, and show the relation between the new spectral types and the natural groups defined by the Palomar-Green (PG) survey.

Key words. stars: early-type – subdwarfs – stars: atmospheres

1. Introduction

We begin with a few words about spectral classification and its role with respect to the fine analysis of stellar spectra. Nobody will deny the importance of classifying astronomical objects on the basis of observable characteristics. What is not always appreciated, however, is the significance of exploiting the classification process to its full potential, as it is in the MK system of spectral classification (Morgan et al. 1943; Walborn 1971; Keenan 1987). As an example, consider the visual comparison of two spectra. One can tell very quickly from visual inspection if the two spectra are identical, to within the errors of observation, and one can predict the outcome of a fine analysis of the second spectrum if one has already been performed on the first (i.e. there will be no significant difference between the results of the two analyses). Furthermore, one normally does not need spectra of as high a resolution as that required to do a fine analysis to come to this conclusion, as blended lines are nearly as useful as unblended ones in determining whether the two spectra are identical, whereas blended lines are nearly useless in performing a fine analysis (although this problem can in principle be solved through the use of synthetic spectra). Finally, one can conclude that the atmospheres of two stars which have slightly different line strengths differ only slightly in their atmospheric properties, since the number of spectral lines is usually much greater than the number of physical parameters characterizing the atmosphere.

Since the spectral resolution of the MK system (2 Å) is sufficient to determine whether the atmospheres of "normal" stars have similar effective temperatures, surface gravities, and chemical compositions, and the differences in the physical parameters characterizing adjacent spectral types are of the same order as the random errors in the determination of these quantities by the fine analysis of 2 Å resolution spectra, an MK spectral type of a "normal" star is, in a sense, equivalent to a fine analysis of a 2 Å resolution spectrum. That this is self-evident is seen by considering that the fine analyses would be done most efficiently by fitting to a model atmosphere grid where the differences in the line strengths of adjacent models were comparable to the random errors in the line strengths, which is also the case with adjacent MK spectral types. For the same reason, fitting to the model grid is, in a sense, equivalent to classifying the spectra using the models as standard spectra. Moreover, because the method of fine analysis depends on the theory of stellar atmospheres, and on the physics underlying it, a fine analysis needs to be redone whenever there are significant advances in the theory, whereas the MK spectral type, which is defined by standard stars, does not change as long as the star itself does not change. Of course, the calibration of the spectral types in terms of physical quantities must be redone whenever there are significant advances in the theory, but this is much easier than redoing the fine analysis for every star. Finally, because spectral classification is independent of the theory of stellar atmospheres, it provides a test of the theory and its underlying physics. Explaining the small changes in line strength as we move between adjacent classes in the MK system is just as valid a test of the theory of stellar atmospheres as explaining the line-to-line variations in the spectrum of a single star. In fact, the MK system itself may

⋆ The normalized, unsmoothed spectra used in this paper are available at the CDS via anonymous ftp to cdsarc.u-strasbg.fr (130.79.128.5) or via http://cdsarc.u-strasbg.fr/viz-bin/qcat?J/A+A/551/A31

be considered to be a kind of hyper-spectrum, which contains within it the spectroscopic constraints to the theory of stellar evolution for "normal" stars (main-sequence stars, giants, and supergiants with atmospheric composition similar to the sun).

It is also of interest that there are similarities in the methodology of both the fine analysis of a spectrum and spectral classification. One does not base a fine analysis on a computer program which blindly matches up local minima in the energy distribution with the wavelengths of all known spectral lines, but rather demands consistency between the strengths of all lines used in the analysis and the results of the analysis, i.e. that all of the strongest lines be present in a given multiplet, and in other multiplets of similar excitation energy for the same ion, and that the effective temperatures, surface gravities, and abundances derived from different lines be in agreement. In classifying the spectrum, we also demand this global consistency: the spectral class must be consistent with all of the lines present in the spectrum, and all of the line strengths must agree with those of the standard to within the observational errors.

It is this last criterion which gives spectral classification one of its most important characteristics: its ability to separate out stars which do not have "normal" spectra, i.e. stars which are not identical to one of the MK standards to within the errors of observation. We are then able to use the method of fine analysis to try to explain how the atmospheres of these "peculiar" stars are different physically from the MK standards. Eventually, it may happen that the number of stars with a given peculiarity becomes so large that it is necessary to set up a new system of spectral classification which incorporates them. The development of new systems of spectral classification which supplement the MK system in this way is an example of the MK process (Morgan 1984).

The hot subdwarfs do not at present fall within the framework of the MK system, i.e. they are "peculiar" stars, and all advances in the understanding of their atmospheres to date have come from model-atmosphere analyses. Green et al. (1986) defined a system of eight classes based on the two dimensions of the HeI/HeII and H/He line strengths. Because the differences in the physical characteristics of adjacent classes were large compared to the errors in the determination of these quantities by fine analysis, and because the number of known hot subdwarfs (more than 3000 at present) was much larger than the number of spectral classes, Drilling (1996) pointed out the need for an MK-like system for the classification of hot subdwarf spectra, and outlined how such a system might be set up. Jeffery et al. (1997) used a preliminary version of this system to classify spectra of one of the eight classes described above (sdOD). In this paper, we attempt to define the system, which has been greatly refined and expanded using a much larger sample of stars distributed over all eight of the Green et al. classes.

2. Observations

The sample of stellar spectra which we consider here is described in detail in a series of papers (Moehler et al. 1990a,b, 1994; Dreizler et al. 1990; and Theissen et al. 1993, 1995) where many of them have been analyzed using model atmospheres. Most of the stars observed were selected from the sample of Green et al. (1986) and may be considered to be a more-or-less representative sample of the Green et al. hot subdwarfs and blue horizontal-branch stars. Most of these spectra cover the wavelength region from 4050 to 4900 Å at a resolution of 2.5 Å. In addition, spectra of nearly all stars classified by Green et al. as sdOD have been included using the similar spectra described by Jeffery et al. (1997). Spectra contaminated with lines from a cooler companion have been eliminated from the sample. All spectra were normalized to the continuum, shifted in wavelength to zero radial velocity, and smoothed to the lowest instrumental resolution used (2.5 Å).

3. Standards and spectral classification

It has been said many times that a system of spectral classification should be defined by the spectra of standard stars, because the system will then be completely independent of the theory of stellar atmospheres and the laws of physics, and can thus serve as a check and a guide to the theory. Indeed, one of the great triumphs of the theory of stellar atmospheres was its success in explaining the gradual variations in line strength as we move through the MK spectral and luminosity sequences. The classification of a star on the MK system is accomplished by comparing its spectrum with those of standard stars. Since the MK system was set up using photographic plates as detectors, it was necessary to obtain spectrograms of all stars, including the standards, with the same equipment and at similar exposure level and air mass in order to do accurate classification. In fact, the classifier needs to use the spectra of as many of the standard stars as possible in determining the spectral type of a given star in order to (a) take into account random errors in the line strengths; (b) ascertain the relative importance of the lines in determining the spectral type; and (c) determine whether or not the spectrum contains any significant peculiarities. It is for these reasons that spectral classification is very difficult to program a computer to do, although this is going to have to be done in order to analyze the very large number of spectra being obtained in current surveys. Encouraging progress along these lines is being made by Winter et al. (2004, 2006). The best classification is not obtained by picking the standard which the star matches most closely, but rather by comparing the strengths of all of the lines in the spectrum of the star to the strengths of all of the lines in all of the standard spectra. A numerical analog of this process is the interpolation of a tabulated quantity using a scheme which makes use of all of the entries in the table.

Since the introduction of linear detectors, it has been possible to do a pretty good job of classifying by comparing spectra taken with different instruments at different locations but with the same resolution and signal-to-noise, although optical or detector differences may still affect the overall appearance or individual features, and continuum normalization and different rebinning/smoothing algorithms can alter the line ratios. The advantage of digital data, in addition to sky subtraction, is the capability of adjusting resolution, line broadening, S/N, and continuum gradients to improve the matching. Therefore, the digital atlas published by Walborn & Fitzpatrick (1990) and the MK standard spectra available on Richard Gray's website[1] proved to be very useful in attempting to interface the hot subdwarf classification described below with the MK system.

The actual procedure to be followed in classifying stellar spectra is not well described in the literature, but we have found it useful to arrange all of the spectra, including the standards, in sequences according to the line strengths, and to then assign a class based on the position of the star in this sequence. This procedure can also be used to set up a new system of classification, and it is greatly facilitated by the ability to display large numbers of spectra simultaneously on a computer screen. As a starting point, we arranged all of the spectra according to the increasing line depths of the Balmer lines (which was historically the

[1] http://stellar.phys.appstate.edu

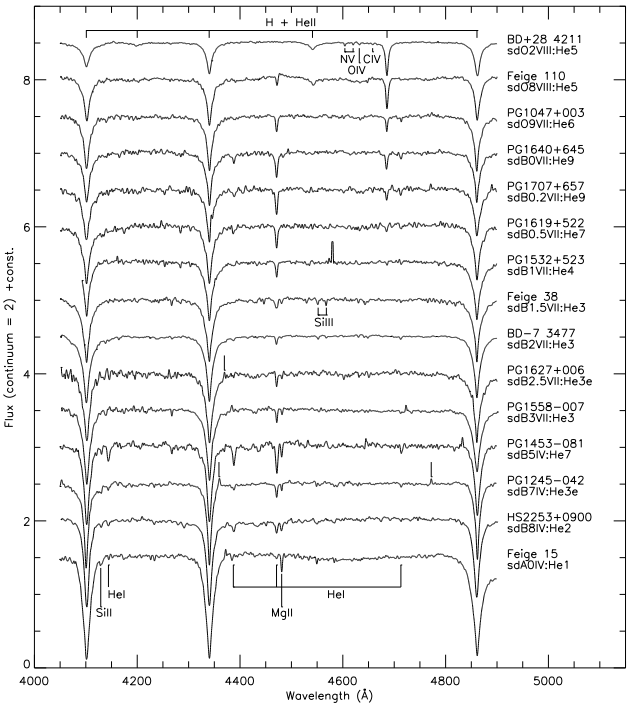

Fig. 1. Spectra of He-normal stars for which hydrogen is dominant and either helium lines of both ionization states or metallic lines are visible. The lines marked are H + HeII $\lambda\lambda$ 4101, 4340, 4861; HeII $\lambda\lambda$ 4200, 4541, 4686; NV λ 4604–20; OIV λ 4632; CIV λ 4658 blend; SiIII λ 4552–68; HeI $\lambda\lambda$ 4144, 4387, 4471, 4713; SiII λ 4128–30; MgII λ 4481; and $\lambda\lambda$ 4360, 4369, 4772 emission.

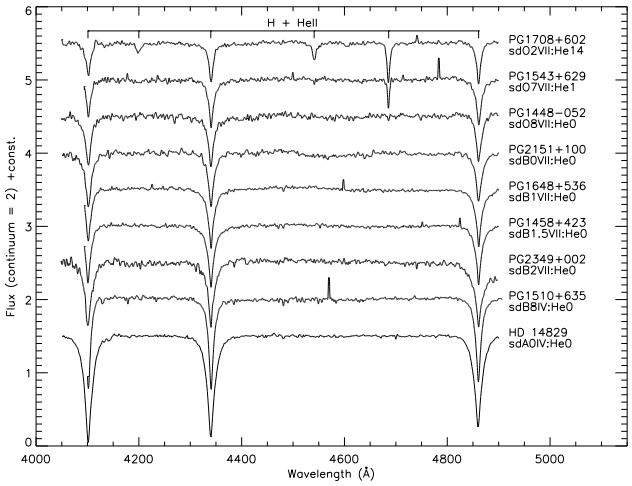

Fig. 2. Spectra of He-weak stars for which hydrogen is dominant and helium lines of only one ionization state may be visible. Metallic lines are very weak or absent. Note that PG1708+602 fits this definition even though the helium class is much higher than those of the other stars. The lines marked are H + HeII $\lambda\lambda$ 4101, 4340, 4861; and HeII $\lambda\lambda$ 4200, 4541, 4686.

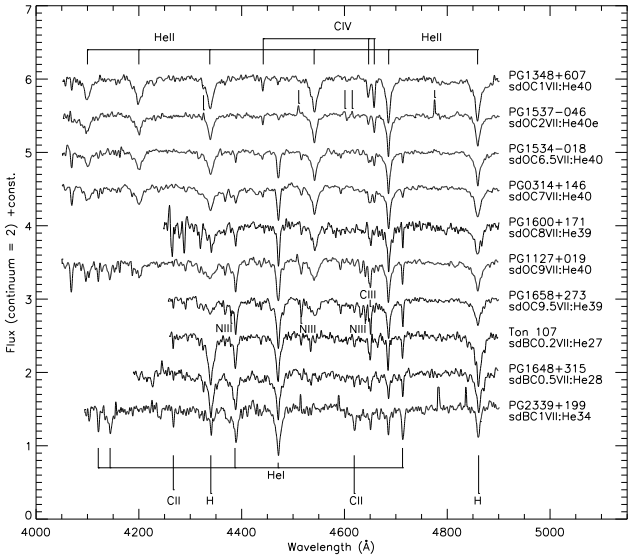

Fig. 3. Spectra of He-strong C stars for which helium is dominant and carbon present. The lines marked are HeII $\lambda\lambda$ 4100, 4200, 4338, 4541, 4686, 4859; CIV $\lambda\lambda$ 4442, 4647, 4658; CIII λ 4650 blend; NIII $\lambda\lambda$ 4379, 4511–15, 4640 blend ; HeI $\lambda\lambda$ 4121, 4144, 4387, 4471, 4713; CII $\lambda\lambda$ 4267, 4619; H $\lambda\lambda$ 4340, 4861; and $\lambda\lambda$ 4326, 4510–11, 4599−4600, 4615, 4776 emission.

starting point for the MK system). When we did this, the other lines did not vary in a gradual manner, presumably due to the fact that the spectral lines are affected by more than one physical parameter in the atmospheres of hot subdwarfs. After much experimentation, it became clear that the spectra could be arranged into sequences where the lines did vary in a gradual manner if the spectra were broken into the following four categories:

1. *He-normal*: spectra dominated by hydrogen lines in which metallic lines or lines due to both HeI and HeII are visible.
2. *He-weak*: spectra containing only hydrogen lines or hydrogen plus either HeI or HeII (but not both). Metallic lines are very weak or absent.
3. *He-strong C*: spectra dominated by helium lines in which carbon lines are present.
4. *He-strong*: spectra dominated by helium lines in which carbon lines are very weak or absent.

We then chose a number of stars from each of these four sequences which we felt best represented the changes within each sequence to serve as standards for the new system. These spectra are displayed in Figs. 1–9, and the apparent *B* magnitudes, equatorial coordinates and spectral types (from this paper) of all of the standards are given in Table 1. Note that the PG designations used in Table 1 and elsewhere in this paper are those given on the finding charts of Green et al. (1986), i.e. with the coordinates given by Green et al. (1986) truncated after minutes of right ascension and rounded off to the nearest tenth of a degree in declination. The J2000 coordinates and *B* magnitudes given in Table 1 were taken from the database described by Østensen (2006) whenever possible, or from SIMBAD. A colon after the *B* magnitude indicates that it is the value given by Green et al. (1986). Emission lines are marked in Figs. 1–9 if they appear in more than one spectrum of the same star. With the exception of the CIII λ 4650 blend, we have not been able to identify these lines from published high-resolution spectra of similar stars, and studies at much higher resolution will be required to identify them.

Since the variations which occur within each sequence are similar to those which occur in MK standards of spectral classes O and B, we use the MK spectral subclasses to identify the subclasses within each sequence. We have attempted to match the new subclasses with the MK subclasses in such a way that the new system merges smoothly with the MK system, so that the two systems can in the future be combined into a single system. Note that this was done before the recent

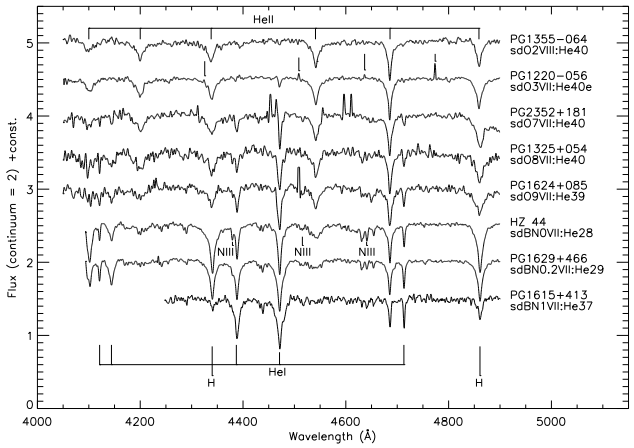

Fig. 4. Spectra of He-strong stars for which helium is dominant and carbon is very weak or absent. NIII may be present. The lines marked are HeII $\lambda\lambda$ 4100, 4200, 4338, 4541, 4686, 4859; NIII $\lambda\lambda$ 4379, 4511–15, 4640 blend ; HeI $\lambda\lambda$ 4121, 4144, 4387, 4471, 4713; H $\lambda\lambda$ 4340, 4861; and $\lambda\lambda$ 4324, 4509, 4637, 4774 emission.

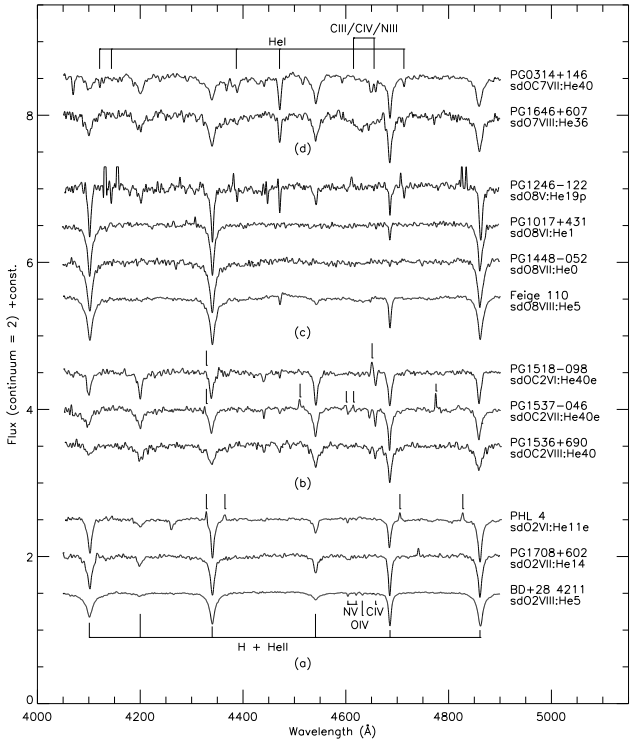

Fig. 5. Luminosity effects for **a)** H-strong sdO2 stars; **b)** He-strong sdO2 stars; **c)** H-strong sdO8 stars; and **d)** He-strong sdO7 stars. The lines marked are HeI $\lambda\lambda$ 4121, 4144, 4387, 4471, 4713; CIII/CIV/NIII λ 4630 broad absorption feature; NV λ 4604-20; OIV λ 4632; CIV λ 4658 blend; H + HeII $\lambda\lambda$ 4101, 4340, 4861; HeII $\lambda\lambda$ 4200, 4541, 4686; and $\lambda\lambda$ 4325–9, 4365, 4510–11, 4599–4601, 4615, 4651, 4705, 4776, 4828 emission.

revisions to the MK system by Sota et al. (2011). Note also that a new subclass, O1, has been created in order to accomplish this end. For the time being, the distinction between the new system and the MK system is denoted by using "sdO" and "sdB" instead of "O" and "B" to denote the spectral class, even though a number of stars classified are not subdwarfs, but related objects such as blue horizontal-branch stars. We identify to which of the above sequences a given star belongs with an "He" designation

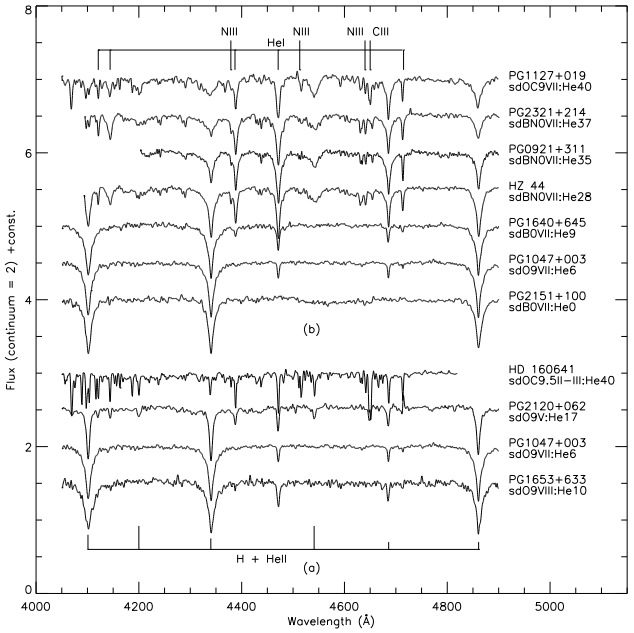

Fig. 6. **a)** Luminosity effects at sdO9; **b)** abundance effects at sdO9 – sdB0. The lines marked are HeI $\lambda\lambda$ 4121, 4144, 4387, 4471, 4713; NIII $\lambda\lambda$ 4379, 4511–15, 4640 blend; CIII λ 4650 blend; H + HeII $\lambda\lambda$ 4101, 4340, 4861; and HeII $\lambda\lambda$ 4200, 4541, 4686.

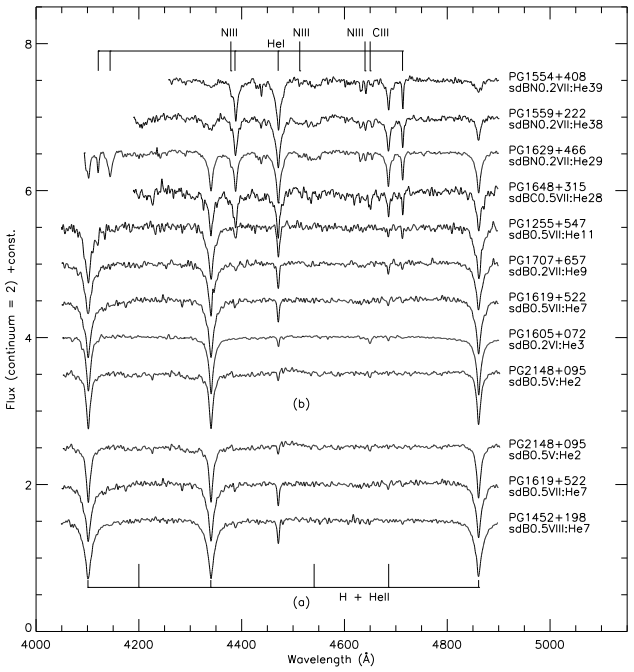

Fig. 7. **a)** Luminosity effects at sdB0.5; **b)** abundance effects at sdB0.2 – sdB0.5. The lines marked are the same as in Fig. 6.

following the spectral class, here an integer from 0 to 40 denoting the strengths of the helium lines relative to the Balmer lines of hydrogen. The helium class is *roughly* equal to the following function of the line depths:

$$20\,\frac{\text{HeI }\lambda4471 + \text{HeII }\lambda4541}{\text{H}\gamma - 0.83\ \text{HeII }\lambda4541}$$

for helium classes 0–20, and

$$40 - 20\,\frac{\text{H}\gamma - 0.83\ \text{HeII }\lambda4541}{\text{HeI }\lambda4471 + \text{HeII }\lambda4541}$$

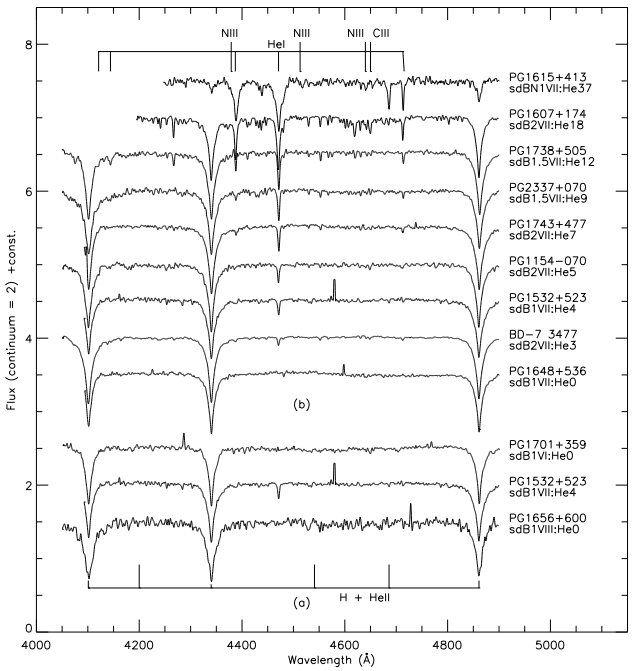

Fig. 8. a) Luminosity effects at sdB1; **b)** abundance effects at sdB1 – sdB2. The lines marked are the same as in Fig. 6.

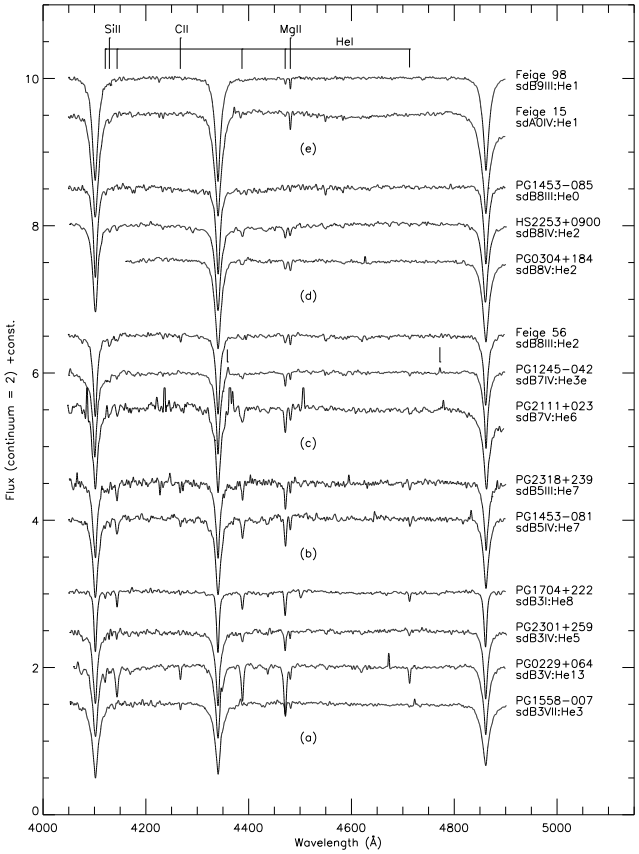

Fig. 9. Luminosity effects at **a)** sdB3; **b)** sdB5; **c)** sdB7-B8; **d)** sdB8; and **e)** sdB9-A0. The lines marked are HeI $\lambda\lambda$ 4121, 4144, 4387, 4471, 4713; SiII λ 4128-30; CII λ 4267; MgII λ 4481; and $\lambda\lambda$ 4358, 4772 emission.

for helium classes 20–40. The term −0.83 HeII λ4541 is an empirical correction for the contribution of the Pickering series of HeII to the depth of Hγ. We denote spectra from the third group by including the letter "C" in the spectral class to identify them as spectra showing strong carbon lines. Finally, we note that the hydrogen and helium line *widths* seem to vary smoothly throughout each sequence, so we have appended "luminosity" class "VII" to most of the hot subdwarfs. If the lines are significantly narrower than average (but still significantly wider than for MK class "V" stars), we append luminosity class "VI" instead, and if the lines are significantly wider than the average, we use luminosity class "VIII". Because most of the hot subdwarfs follow the average trend (luminosity class VII), we do not feel that a more detailed "luminosity" classification for them is is justified at the present time. Stars given luminosity classes I–V were classified using MK standards. Note that the term luminosity class is something of a misnomer, as the physical quantity upon which the luminosity class is dependent is the surface gravity, and not the luminosity. This point is discussed further in Sect. 4. A detailed description of the standard spectra displayed in Figs. 1–9 follows:

1. *He-normal* (strong hydrogen, metallic lines or both HeI and HeII present): it is for the stellar spectra shown in Fig. 1 that we see variations very similar to those for MK luminosity class V. We chose BD+28 4211 as the standard for spectral class sdO2, since it shows weak lines of NV, OIV and CIV, but no trace of HeI at this resolution, which is consistent with the definition of spectral class O2 given by Walborn et al. (2002). From O2 through B1, the principal criterion for the spectral class is HeI λ 4471/HeII λ 4541. Because of the weakness of the Pickering series in subdwarfs of these spectral classes, we use HeI λ 4471/HeII λ 4686, which is affected somewhat by the luminosity class, as a secondary criterion. From O8 to B1, HeI λ 4713/HeII λ 4686 can also be used. From B0.5 through A0, the primary criteria are SiIII/HeI, MgII/HeI and SiII/HeI. Again, these criteria have been adjusted so that the line ratios defining each spectral class are roughly the same as they are in normal stars of the same MK spectral class at luminosity class V. Note that the *depths* of the Balmer lines increase downwards through the sequence. This is of critical importance, since we are going to be forced to use the depths of the Balmer lines as the primary indicator of spectral class in the next sequence.
2. *He-weak* (strong hydrogen, lines of HeI and HeII not simultaneously present, metallic lines very weak or absent): in Fig. 2, the spectra are arranged in the order of increasing depths of the Balmer lines. This is the only indicator of spectral class, and the classes are assigned such that stars which have the same Balmer line depths in Figs. 1 and 2 have the same spectral class.
3. *He-strong C* (helium dominant, carbon present): in Fig. 3, we see that from OC1 through OC2, lines due to CIV and the HeII Pickering series are all strong and decrease in strength. HeI λ 4471 is very weak, as it is in MK class O3 as defined by Walborn and Fitzpatrick (1990). One must bear in mind, however, that this line would be invisible if helium were as weak in these spectra as in normal main-sequence stars. From OC2 to BC1, we take the ratio of the line depths of HeI λ 4471 and HeII λ 4541 as the principal criterion for the spectral class, with the correspondence between that line ratio and spectral class being roughly the same as that for normal stars of MK luminosity class V. Secondary criteria are HeI λ 4713/HeII λ 4541, CIV/CIII (for spectral classes OC2 through OC9), CII/CIII (for spectral

Table 1. Standard stars defining the new system.

Star	B	RA(J2000)	Dec(J2000)	Spectral type
PG1348+607	16.04	13 50 15.98	+60 24 38.4	sdOC1VII:He40
PHL 4	14.83	21 26 21.16	+00 58 35.1	sdO2VI:He11e
PG1518−098	13.50	15 20 59.34	−09 58 55.9	sdOC2VI:He40e
PG1708+602	13.15	17 09 15.90	+60 10 10.8	sdO2VII:He14
PG1537−046	14.82	15 40 33.34	−04 48 12.4	sdOC2VII:He40e
BD+28 4211	10.18	21 51 11.05	+28 51 50.9	sdO2VIII:He5
PG1355−064	12.79	13 57 54.34	−06 37 31.6	sdO2VIII:He40
PG1536+690	14.35	15 36 48.83	+68 52 08.6	sdOC2VIII:He40
PG1220−056	14.44	12 22 58.97	−05 53 04.9	sdO3VII:He40e
PG1534−018	14.82	15 37 33.80	−02 00 21.9	sdOC6.5VII:He40
PG1543+629	14.60	15 44 38.15	+62 43 24.3	sdO7VII:He1
PG2352+181	13.08	23 55 17.24	+18 20 15.6	sdO7VII:He40
PG0314+146	12.89	03 17 38.05	+14 46 25.7	sdOC7VII:He40
PG1646+607	16.27:	16 46 44.30	+60 37 09.2	sdO7VIII:He36
PG1246−122	14.39	12 49 21.67	−12 29 32.0	sdO8V:He19p
PG1017+431	14.82	10 20 29.83	+42 50 22.0	sdO8VI:He1
PG1448−052	14.76	14 51 13.12	−05 23 16.9	sdO8VII:He0
PG1600+171	16.49	16 03 04.10	+16 59 54.4	sdOC8VII:He39
PG1325+054	14.07	13 28 21.40	+05 08 55.8	sdO8VII:He40
Feige 110	11.51	23 19 58.41	−05 09 55.8	sdO8VIII:He5
PG2120+062	14.20	21 22 31.72	+06 21 56.2	sdO9V:He17
PG1047+003	13.18	10 50 02.86	−00 00 35.0	sdO9VII:He6
PG1624+085	14.57	16 26 54.22	+08 25 35.6	sdO9VII:He39
PG1127+019	13.01	11 30 03.72	+01 37 37.6	sdOC9VII:He40
PG1653+633	15.78	16 54 22.27	+63 15 34.8	sdO9VIII:He10
HD 160641	10.01	17 41 51.48	−17 53 48.5	sdOC9.5II-III:He40
PG1658+273	15.73:	17 00 14.23	+27 12 37.3	sdOC9.5VII:He39
PG2151+100	12.46	21 53 57.23	+10 17 37.7	sdB0VII:He0
PG1640+645	15.17:	16 40 50.69	+64 24 45.3	sdB0VII:He9
HZ 44	11.44	13 23 35.17	+36 08 00.3	sdBN0VII:He28
PG0921+311	14.19	09 24 40.05	+30 50 13.1	sdBN0VII:He35
PG2321+214	12.89:	23 24 27.40	+21 38 51.6	sdBN0VII:He37
PG1605+072	12.78	16 08 03.70	+07 04 29.1	sdB0.2VI:He3
PG1707+657	15.91	17 07 14.28	+65 40 25.3	sdB0.2VII:He9
PG1559+048	14.29	16 01 31.32	+04 40 27.1	sdBC0.2VII:He22
Ton 107	16.55	12 42 01.78	+43 40 24.4	sdBC0.2VII:He27
PG1629+466	14.04:	16 31 17.75	+46 31 00.4	sdBN0.2VII:He29
PG1559+222	14.50	16 01 13.81	+22 05 46.5	sdBN0.2VII:He38
PG1554+408	15.88	15 55 50.40	+40 38 53.9	sdBN0.2VII:He39
PG2148+095	13.00	21 51 16.87	+09 46 59.7	sdB0.5V:He2
PG1619+522	13.08	16 20 38.74	+52 06 08.8	sdB0.5VII:He7
PG1255+547	13.12	12 57 49.55	+54 25 35.0	sdB0.5VII:He11
PG1648+315	15.97	16 50 22.03	+31 27 49.8	sdBC0.5VII:He28
PG1452+198	12.03	14 54 39.80	+19 37 00.9	sdB0.5VIII:He7
PG1701+359	13.07	17 03 21.67	+35 48 48.4	sdB1VI:He0
PG1648+536	14.35	16 49 59.86	+53 31 32.7	sdB1VII:He0
PG1532+523	13.83	15 33 29.84	+52 06 50.0	sdB1VII:He4
PG2339+199	15.78:	23 41 56.69	+20 12 22.7	sdBC1VII:He34
PG1615+413	16.64:	16 17 40.15	+41 12 52.4	sdBN1VII:He37
PG1656+600	15.90:	16 56 50.17	+59 55 42.0	sdB1VIII:He0
PG1458+423	13.55	15 00 24.61	+42 05 45.5	sdB1.5VII:He0
Feige 38	12.77	11 16 49.66	+06 59 30.8	sdB1.5VII:He3
PG2337+070	13.29	23 40 04.82	+07 17 11.0	sdB1.5VII:He9
PG1738+505	13.08	17 39 28.43	+50 29 25.1	sdB1.5VII:He12
PG2349+002	13.05	23 51 53.26	+00 28 18.0	sdB2VII:He0
BD−7 3477	10.27	12 44 20.21	−08 40 15.9	sdB2VII:He3
PG1154−070	14.18	11 57 03.61	−07 17 30.0	sdB2VII:He5
PG1743+477	13.41	17 44 26.41	+47 41 46.3	sdB2VII:He7
PG1607+174	11.88	16 09 54.94	+17 14 57.9	sdB2VII:He18
PG1627+006	14.71	16 29 35.90	+00 31 49.4	sdB2.5VII:He3e
PG1704+222	12.83	17 06 46.18	+22 05 52.2	sdB3I:He8
PG2301+259	12.99	23 04 17.24	+26 12 02.9	sdB3IV:He5
PG0229+064	11.50	02 32 36.26	+06 38 52.2	sdB3V:He13
PG1558−007	13.48	16 01 14.04	−00 51 41.6	sdB3VII:He3
PG2318+239	14.40	23 21 05.80	+24 10 39.2	sdB5III:He7
PG1453−081	13.91	14 56 00.32	−08 15 49.0	sdB5IV:He7

Table 1. continued.

Star	B	RA(J2000)	Dec(J2000)	Spectral type
PG1245−042	13.31	12 48 13.94	−04 30 47.4	sdB7IV:He3e
PG2111+023	13.01	21 13 42.34	+02 33 10.2	sdB7V:He6
PG1453−085	12.75	14 56 27.40	−08 44 22.9	sdB8III:He0
Feige 56	10.92	12 06 47.23	+11 40 12.7	sdB8III:He2
PG1510+635	14.00	15 11 10.29	+63 21 49.6	sdB8IV:He0
HS2253+0900	13.94	22 55 50.94	+09 17 01.6	sdB8IV:He2
PG0304+184	12.36	03 07 47.44	+18 33 28.8	sdB8V:He2
Feige 98	11.74	14 38 15.77	+27 29 33.0	sdB9III:He1
HD 14829	10.31	02 23 09.25	−10 40 39.3	sdA0IV:He0
Feige 15	10.44	01 49 09.48	+13 33 11.8	sdA0IV:He1

classes OC9 through BC1), and the absolute strengths of the NIII lines (for spectral classes OC6.5 through BC1). The similarity of these variations to the MK temperature sequence suggests that the variations in the helium, carbon, and nitrogen lines are primarily due to a decrease in the effective temperatures of the corresponding stellar atmospheres as we move from the top to the bottom of the sequence. This point is discussed further in Sect. 4.

4. *He-strong* (helium dominant, carbon weak or absent): in Fig. 4, we see that spectra of stars of a given spectral class appear to be identical to stars of the same spectral class in Fig. 3, except for the carbon lines, which are weak or absent. This would suggest that these stars have a carbon abundance significantly lower than stars of the same spectral class in Fig. 3, which are designated by a "C" in the spectral class. If CIII is weak or absent and NIII is visible, we use sdBN in the spectral class in order to be consistent with the definition of OBN stars given by Walborn (1976).

In Fig. 5, we show luminosity and abundance effects for stars earlier than spectral class sdO9. These stars tend to be either H-strong (helium class less than 15) or extremely He-strong (helium class 40). Note the increased broadening of the H and He lines and the increase in the HeII λ 4686 line depth relative to the Pickering series of HeII as we move from luminosity class V to luminosity class VIII at spectral class sdO2-sdO8. Note also the emission reversal of the CIII λ 4650 blend at luminosity class VI for the sdOC2 stars. We may be seeing here, and in some of the other emission features marked, the same type of NLTE effects seen in the O supergiants and in main-sequence stars near spectral class O4 (see Walborn & Fitzpatrick 1990; Walborn et al. 2010) in these even hotter O-type subdwarfs. At sdO7, luminosity class VIII is distinguished from luminosity class VII in the He-strong stars by the increased strength of HeII λ 4686 relative to the other helium lines and by the broad feature centered near λ 4630, which is due to CIII, CIV, and NIII (Dreizler, priv. comm.).

Similar effects are present at spectral class sdO9, as shown in Fig. 6. We have included a spectrum of the post-EAGB star PG2120+062 (Moehler et al. 1994) to show how it fits into this scheme, and of the very narrow-lined extreme helium star HD160641 (Bidelman 1952) to show how these stars may be considered to be the low surface-gravity counterparts of the extremely He-strong subdwarfs. We also show a series of sdO9VII – sdB0VII stars of increasing helium class in Fig. 6. Notice that unlike the sdO stars, the intermediate helium classes for the sdB0 stars are now starting to fill in at He35 (PG0921+311) and He28 (HZ 44). These intermediate helium classes continue to fill in from sdB0.2 to sdB2, as shown in Figs. 7 and 8. We also show luminosity effects for sdB0.5 and sdB1.

The broadening of the Balmer lines with increasing luminosity class is shown for the H-strong sdB3 stars in Fig. 9. At later spectral types we find only blue horizontal-branch stars, which we have essentially classified using MK standards (except for the helium class).

Finally, we use the standard spectra listed in Table 1 and shown in Figs. 1–9 to classify all of the spectra in our sample. The results are given in Table 2. A "p" is appended to the spectral type to indicate a peculiarity described in the remarks to Table 2, and an "e" is appended if emission features were present in more than one spectrum of the same star. Note that the emission features have been clipped at 15 percent above the continuum in Figs. 1–9. The mean errors of classification, as estimated from the results for stars for which we have more than one spectrum, are ±0.4 spectral classes, ±0.2 luminosity classes, and ±1.1 helium classes.

4. Calibrations

As mentioned earlier, model-atmosphere analyses have been carried out for a large number of these spectra (in fact, this was the primary reason for obtaining the spectra used for the spectral classification). We have not used the results of Moehler et al. (1990b) or Theissen et al. (1993) in the calibrations, as colors were used in these analyses to determine the effective temperatures, and the effective temperature versus color calibration used (Lester et al. 1986) is not valid for O and B subdwarfs (Napiwotzki et al. 1993). We also did not use the results of Saffer et al. (1994) in the calibrations because they are based on spectra of a much lower (and variable) resolution and because the analyses did not account for metallic line blanketing. The spectral classification itself proved to be a very useful tool in deciding which results to use in the calibrations, as the spectral types can be used to compare the results of different workers even though they have no stars in common, and plots of the atmospheric parameters versus spectral type revealed significant systematic differences between our final calibrations and the results cited above. The results upon which our final calibrations are based are given in Table 3, and there appear to be no significant systematic differences between them.

The scheme of spectral classification which we have just set up in an empirical fashion, completely independent of the theory of stellar atmospheres, suggests that the sequences which we have identified are temperature sequences which differ primarily in the H/He and C/He abundance ratios. This is supported by the calibrations given in Figs. 10 and 11, in which the effective temperatures from Table 3 are plotted against spectral class. The straight line fit shown in Fig. 10,

$$T_{\rm eff}[{\rm K}] = 74\,900 - 4030\,s,$$

Table 2. Spectral types for all stars in our sample.

Star	Spectral type	Star	Spectral type	Star	Spectral type
PG0001+275	sdB2VII:He3	PG1426−067	sdO8VIII:He0	PG1715+273	sdB1VII:He35
PG0004+133	sdB2.5V:He7	PG1432+004	sdB2VII:He6	PG1716+426	sdB2VII:He3
PG0009+036[a]	sdB2VII:He4p	PG1433+240	sdB2VII:He4	PG1722+286[q]	sdB0VII:He10p
PG0039+135	sdOC7VII:He40	PG1441+407	sdO7VII:He40	PG1724+590	sdB2VII:He5
PG0057+155[b]	sdB0.2VIII:He8p	PG1448−052	sdO8VII:He0	PG1725+252	sdB1.5VII:He2
PG0101+040	sdB2VII:He4	PG1451+492	sdB3VI:He6	PG1738+505	sdB1.5VII:He12
PG0133+114	sdB1.5VII:He4	PG1452+198	sdB0.5VIII:He7	PG1739+489	sdB2VII:He3
PG0135+243	sdBC1V:He35	PG1453−081	sdB5IV:He7	PG1743+477	sdB2VII:He7
PG0142+148	sdB2VI:He2	PG1453−085	sdB8III:He0	PG2059+013	sdB1VI:He13
PG0208+016	sdO9VII:He39	PG1458+423	sdB1.5VII:He0	PG2111+023	sdB7V:He6
PG0209−015	sdB3VII:He4	PG1506−052	sdO7VI:He1	PG2120+062	sdO9V:He17
PG0229+064	sdB3V:He13	PG1510+635	sdB8IV:He0	PG2148+095	sdB0.5V:He2
PG0240+046	sdBC0.2VII:He24	PG1518−098[j]	sdOC2VI:He40e	PG2151+100	sdB0VII:He0
PG0242+132	sdB0.5V:He10	PG1519+640	sdB1.5VII:He5	PG2158+082	sdO2VIII:He40
PG0304+184	sdB8V:He2	PG1526+440	sdBC0.2VII:He26	PG2159+051	sdB7III:He3
PG0314+146	sdOC7VII:He40	PG1532+523	sdB1VII:He4	PG2204+035	sdB1VII:He10
PG0314+180[b]	sdO3VIII:He1p	PG1534−018	sdOC6.5VII:He40	PG2205+023[b]	sdB2VIII:He0p
PG0342+026	sdB3VII:He4	PG1536+690	sdOC2VIII:He40	PG2215+151	sdOC9VII:He40
PG0838+133	sdOC7VII:He40	PG1537−046[k]	sdOC2VII:He40e	PG2218+020	sdB2.5VII:He3
PG0856+121	sdB3VII:He0	PG1538+401	sdO9VIII:He0	PG2219+094[a]	sdB0.5V:He7p
PG0902+058	sdBN0VII:He38	PG1543+629	sdO7VII:He1	PG2229+099	sdB5III:He11
PG0906+597[c]	sdO2VIII:He1	PG1544+488[a]	sdBC1VII:He39p	PG2258+155	sdB0.2VII:He39
PG0907+123	sdB2VI:He2	PG1544+601	sdB1.5VII:He1	PG2259+134	sdB1VII:He9
PG0909+164	sdO8VII:He1	PG1545+035[l]	sdO2VI:He12e	PG2301+259	sdB3IV:He5
PG0909+276	sdB0.5VII:He19	PG1549+006[m]	sdB0.2VI:He7e	PG2314+076[r]	sdB1.5VIII:He0p
PG0918+029	sdB1VII:He6	PG1553−077[n]	sdOC7VII:He40e	PG2317+046	sdO8VII:He1
PG0920+029	sdB2VI:He3	PG1554+408	sdBN0.2VII:He39	PG2318+239	sdB5III:He7
PG0921+161	sdB0VII:He9	PG1558−007	sdB3VII:He3	PG2321+214	sdBN0VII:He37
PG0921+311	sdBN0VII:He35	PG1559+048	sdBC0.2VII:He22	PG2331+038	sdB1.5VII:He2
PG0934+145	sdB5IV:He7	PG1559+222	sdBN0.2VII:He38	PG2337+070	sdB1.5VII:He9
PG0954+049	sdB8III:He2	PG1559+533	sdB2VII:He3	PG2339+199	sdBC1VII:He34
PG1017+431	sdO8VI:He1	PG1600+171	sdOC8VII:He39	PG2345+241	sdB3IV:He12
PG1018−047	sdB2VII:He0	PG1602+013[o]	sdO5VI:He2pe	PG2349+002	sdB2VII:He0
PG1047+003	sdO9VII:He6	PG1605+072	sdB0.2VI:He3	PG2351+198	sdB5III:He4
PG1049+013[d]	sdO8VI:He1pe	PG1607+174	sdB2VII:He18	PG2352+181	sdO7VII:He40
PG1050−065	sdB0.2VII:He12	PG1610+519	sdO8VI:He1	PG2358+107	sdB2VII:He4
PG1118+061	sdB1.5VII:He1	PG1613+467	sdB2VII:He5	BD−7 3477	sdB2VII:He3
PG1127+019	sdOC9VII:He40	PG1615+413	sdBN1VII:He37	BD+25 3941[a]	sdB0.5VI:He9p
PG1136−003[e]	sdB1VII:He1e	PG1618+563	sdB0VII:He8	BD+28 4211	sdO2VIII:He5
PG1154−070	sdB2VII:He5	PG1619+522	sdB0.5VII:He7	Feige 15	sdA0IV:He1
PG1220−056[f]	sdO3VII:He40e	PG1619+525	sdB0.5VIII:He7	Feige 38	sdB1.5VII:He3
PG1230+067	sdBN0VII:He39	PG1624+085	sdO9VII:He39	Feige 56	sdB8III:He2
PG1245−042[g]	sdB7IV:He3e	PG1627+006[p]	sdB2.5VII:He3e	Feige 98	sdB9III:He1
PG1246−122[h]	sdO8V:He19p	PG1627+017	sdB3VII:He3	Feige 110	sdO8VIII:He5
PG1249+762	sdOC2VIII:He36	PG1629+466	sdBN0.2VII:He29	FHB 18	sdA0IV:He0
PG1255+547	sdB0.5VII:He11	PG1640+645	sdB0VII:He9	HD 14829	sdA0IV:He0
PG1258−030	sdB8IV:He1	PG1644+404	sdB1.5VII:He2	HD 160641	sdOC9.5II-III:He40
PG1300+279[a]	sdO6.5VII:He35p	PG1645+610	sdB1VII:He5	HS0016+0044	sdB1.5VII:He2
PG1303−114	sdB0.2VII:He3	PG1646+607	sdO7VIII:He36	HS1000+471	sdBC0.2VII:He28
PG1323−086	sdB3I:He8	PG1648+315	sdBC0.5VII:He28	HS1844+637	sdB1VII:He39
PG1325+054	sdO8VII:He40	PG1648+536	sdB1VII:He0	HS2253+0900	sdB8IV:He2
PG1336−018	sdB1VII:He1	PG1653+633	sdO9VIII:He10	HS2301+0728	sdB8III:He0
PG1343+578[i]	sdB5III:He2p	PG1656+600	sdB1VIII:He0	HZ 15	sdB2II:He15
PG1343−102	sdB1.5VII:He0	PG1658+273	sdOC9.5VII:He39	HZ 44	sdBN0VII:He28
PG1348+607	sdOC1VII:He40	PG1701+359	sdB1VI:He0	LSIV−14 116	sdB0.5VII:He18
PG1352−023	sdO8VIII:He7	PG1704+222	sdB3I:He8	LSIV+6 2	sdBC1V:He39
PG1355−064	sdO2VIII:He40	PG1705+537	sdB5III:He5	LSS 5121	sdBC0II:He40
PG1401+289	sdOC7VII:He40	PG1707+657	sdB0.2VII:He9	PHL 4[s]	sdO2VI:He11e
PG1409−103	sdO5VI:He1	PG1708+142	sdB2.5IV:He11	Ton 107	sdBC0.2VII:He27
PG1413+114	sdOC9.5VII:He39	PG1708+602	sdO2VII:He14		
PG1415+492	sdBC1V:He38	PG1710+490	sdB1.5VII:He3		

Notes. [a] Lines unusually broad; [b] unidentified absorption feature near λ 4500 Å; [c] spectrum very noisy; [d] unidentified broad absorption feature near λ 4265 Å; $\lambda\lambda$ 4326, 4627, 4703 emission; [e] $\lambda\lambda$ 4510, 4671, 4749, 4775 emission; [f] $\lambda\lambda$ 4324, 4509, 4637, 4774 emission; [g] $\lambda\lambda$ 4360, 4772 emission; [h] HeI lines show wind profiles; [i] weak G band? [j] $\lambda\lambda$ 4325, 4651 emission; [k] $\lambda\lambda$ 4326, 4510–11, 4599–4601, 4615, 4776 emission; [l] $\lambda\lambda$ 4508, 4567, 4654–7, 4721, 4758, 4773 emission; [m] $\lambda\lambda$ 4326, 4510, 4704, 4760, 4775 emission; [n] $\lambda\lambda$ 4326, 4383, 4703, 4774 emission; [o] λ 4509 emission; weak G band? [p] $\lambda\lambda$ 4369, 4409, 4792 emission; [q] unidentified absorption feature near λ 4530 Å; broad emission feature near λ 4735 Å; [r] unusually narrow HeI λ 4144 and CII λ 4267; [s] $\lambda\lambda$ 4329, 4365, 4705, 4828 emission.

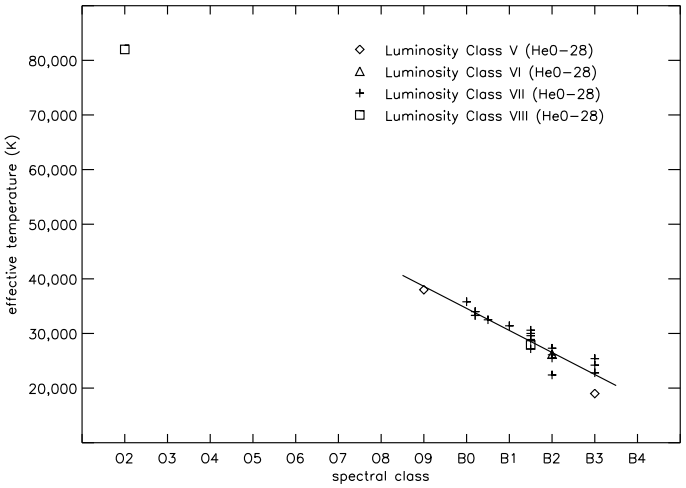

Fig. 10. Effective temperature versus spectral class for helium class 0–28 and luminosity class V–VIII.

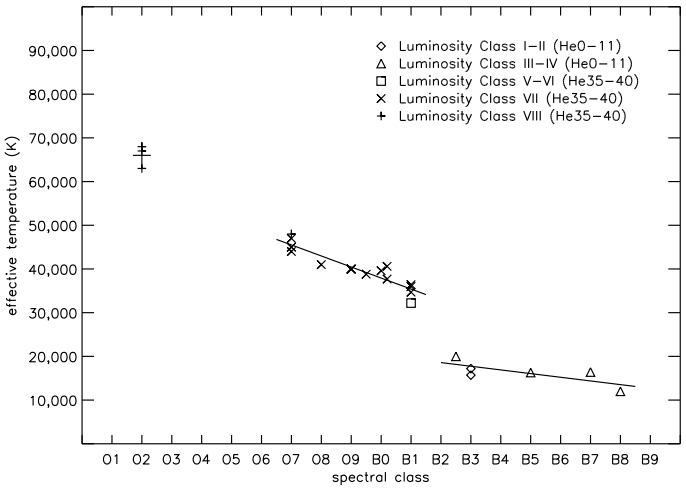

Fig. 11. Effective temperature versus spectral class for helium class 35–40 and luminosity class V–VIII and for helium class 0–11 and luminosity class I–IV. The large cross is the average given in the text.

where s is the spectral subclass for sdO stars and 10 plus the spectral subclass for sdB stars, yields the effective temperatures for hot subdwarfs of spectral class O9–B3, helium class 0–28, and luminosity class V–VIII to a mean error of ±1700 K. There appears to be no correlation of the effective temperature with either helium class or luminosity class within these ranges, although only 5 of the 23 stars plotted have He classes greater than 13. Straight line fits in effective temperature versus spectral class also seem to be adequate for hot subdwarfs of spectral class O7–B1, helium class 35–40, and luminosity class V–VIII,

$$T_{\rm eff}[{\rm K}] = 63\,200 - 2520\ s,$$

to a mean error of ±1600 K, and for stars of luminosity class I–IV, spectral class B2.5–B8, and helium class 0–11,

$$T_{\rm eff}[{\rm K}] = 28\,700 - 841\ s,$$

to a mean error of ±1900 K (see Fig. 11). Again, within the ranges given, there appears to be no correlation of the effective temperature with either helium class or luminosity class. The O2 stars of helium class 36–40 have been calibrated separately from the other types and yield a mean effective temperature of 66 000 K with a mean error of ±2600 K.

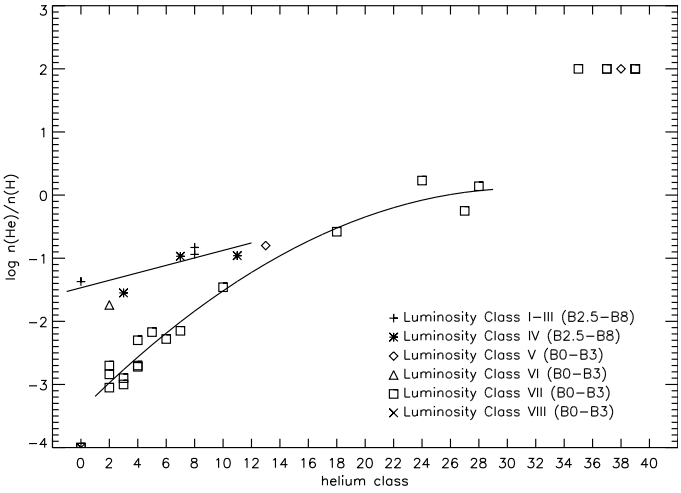

Fig. 12. Helium to hydrogen abundance ratio (by numbers of atoms) versus helium class for sdB0-sdB3 V–VIII and sdB2.5-sdB8 I–IV.

That He-weak stars have low helium abundances, He-normal stars, more nearly solar helium abundances, and He-strong stars, high helium abundances is supported by the calibrations given in Figs. 12 and 13, where the helium abundances given in Table 3 are plotted against helium class. In Fig. 12, the quadratic fit,

$$\log \frac{n({\rm He})}{n({\rm H})} = -3.41 + 0.225\ h - 0.00361\ h^2,$$

where h is the helium class, is seen to be adequate for sdB (sdB0–sdB3 V–VIII) stars with $1 < h < 29$ with a mean error in $\log [n({\rm He})/n({\rm H})]$ of ±0.21. For $34 < h < 40$, $n({\rm H})/n({\rm He})$ is 0.01 with a mean error less than 0.01. The reason for this is that the Hβ line is clearly visible at these spectral classes if even this trace amount of hydrogen is present. For $h = 0$, $\log[n({\rm He})/n({\rm H})] < -4$. Also in Fig. 12, the straight line fit,

$$\log \frac{n({\rm He})}{n({\rm H})} = -1.47 + 0.0592\ h,$$

is seen to be adequate for sdB2.5-sdB8 I–IV stars with $h < 12$, with a mean error of ±0.18. Figure 12 shows that there is a dependence of the helium abundance on luminosity class, and for this reason we have only included stars of luminosity class VII in the sdB calibration.

The situation is much less clear for the sdO stars, as shown in Fig. 13. All but 2 of the stars for which helium abundances are given in Table 3 have $h > 35$, and these are either rather uncertain upper limits ($n({\rm He})/n({\rm H})$ less than 10 or 20) or have very large mean errors. The reason for this is the blending of the Balmer lines with the Pickering series of HeII in the sdO stars, which makes the determination of $n({\rm He})/n({\rm H})$ difficult.

Finally, we plot the surface gravities given in Table 3 against luminosity class in Fig. 14 (helium classes 0–18) and Fig. 15 (helium classes 24–40). The resulting calibrations are given in Tables 4 and 5, respectively. There appears to be no significant dependence of these calibrations on either spectral class or helium class within the ranges given, although it is seen from the figures that the distribution of the points with spectral class is far from uniform, and only 5 of the 50 stars plotted have helium classes of 14–34. We do not consider the calibrations for

Table 3. Atmospheric parameters used in the calibrations.

Star	Ref.	$T_{\rm eff}$ [10^3K]	$\log g$ [cms^{-2}]	log[n(He)/n(H)]	Spectral type	Comments
PG0039+135	1	45.0	5.00	1.00	sdOC7VII:He40	abundance uncertain
PG0101+040	8	27.3	5.50	−2.70	sdB2VII:He4	
PG0133+114	8	29.6	5.66	−2.30	sdB1.5VII:He4	
PG0208+016	1	40.0	5.00	1.00	sdO9VII:He39	abundance uncertain
PG0229+064	9	19.0	4.55	−0.80	sdB3V:He13	
PG0240+046	7	34.0	5.40	0.23	sdBC0.2VII:He24	
PG0342+026	11	25.4	5.44	−2.72	sdB3VII:He4	upper limit to abundance
PG0838+133	1	44.0	4.80	1.00	sdOC7VII:He40	abundance uncertain
PG0856+121	11	24.2	5.47	−4.00	sdB3VII:He0	upper limit to abundance
PG0907+123	6	26.2	5.30	−1.74	sdB2VI:He2	
PG1127+019	7	39.9	5.00	2.00	sdOC9VII:He40	
PG1245−042	10	16.4	3.95	−1.55	sdB7IV:He3e	
PG1249+762	1	68.0	5.80	1.00	sdOC2VIII:He36	lower limit to abundance
PG1323−086	5	15.7	2.35	−0.83	sdB3I:He8	
PG1325+054	1	41.0	5.00	1.30	sdO8VII:He40	lower limit to abundance
PG1401+289	1	47.0	5.50	1.30	sdOC7VII:He40	lower limit to abundance
PG1415+492	7	32.2	4.20	2.00	sdBC1V:He38	
PG1432+004	14	22.4	5.15	−2.28	sdB2VII:He6	
PG1453−081	10	16.3	4.20	−0.97	sdB5IV:He7	
PG1453−085	10	12.0	3.20	−1.37	sdB8III:He0	
PG1519+640	13	30.6	5.72	−2.17	sdB1.5VII:He5	
PG1536+690	1	63.0	5.80	1.00	sdOC2VIII:He40	lower limit to abundance
PG1554+408	7	37.7	5.20	2.00	sdBN0.2VII:He39	
PG1615+413	7	36.0	5.20	2.00	sdBN1VII:He37	
PG1624+085	1	40.0	5.30	1.30	sdO9VII:He39	lower limit to abundance
PG1627+017	6	22.8	5.27	−3.00	sdB3VII:He3	
PG1644+404	14	30.0	5.78	−2.84	sdB1.5VII:He2	
PG1646+607	1	48.0	6.00	0.00	sdO7VIII:He36	
PG1648+536	13	31.4	5.62	−4.00	sdB1VII:He0	upper limit to abundance
PG1658+273	7	38.8	4.90	2.00	sdOC9.5VII:He39	
PG1704+222	5	17.2	2.65	−0.94	sdB3I:He8	
PG1708+142	3	20.0	3.70	−0.96	sdB2.5IV:He11	
PG1715+273	7	34.7	5.00	2.00	sdB1VII:He35	
PG1716+426	8	26.1	5.33	−2.90	sdB2VII:He3	
PG1722+286	6	35.8	5.94	−1.46	sdB0VII:He10p	
PG1725+252	6	28.9	5.54	−3.05	sdB1.5VII:He2	
PG1743+477	6	25.5	5.41	−2.15	sdB2VII:He7	
PG2120+062	4	38.0	4.25	−1.06	sdO9V:He17	assumed solar abundance
PG2158+082	1	67.0	5.50	1.00	sdO2VIII:He40	lower limit to abundance
PG2215+151	1	40.0	5.00	1.00	sdOC9VII:He40	lower limit to abundance
PG2258+155	12	40.6	5.71	2.00	sdB0.2VII:He39	
PG2314+076	14	27.9	5.69	−4.00	sdB1.5VIII:He0p	upper limit to abundance
PG2321+214	7	39.6	5.30	2.00	sdBN0VII:He37	
PG2331+038	13	27.2	5.58	−2.70	sdB1.5VII:He2	
PG2352+181	1	45.0	5.50	1.00	sdO7VII:He40	lower limit to abundance
BD+28 4211	2	82.0	6.20	−1.00	sdO2VIII:He5	
HS1000+471	7	33.3	4.70	0.14	sdBC0.2VII:He28	
HS1844+637	7	36.4	5.10	2.00	sdB1VII:He39	
LSIV−14 116	7	32.5	5.40	−0.58	sdB0.5VII:He18	
Ton 107	7	33.3	5.00	−0.25	sdBC0.2VII:He27	

References. (1) Dreizler et al. (1990); (2) Napiwotzki (1993); (3) Conlon et al. (1993); (4) Moehler et al. (1994); (5) Moehler and Heber (1998); (6) Maxted et al. (2001); (7) Ahmad and Jeffery (2003); (8) Morales-Rueda et al. (2003); (9) Ramspeck et al. (2001); (10) Schmidt (1996); (11) Salomon (2003); (12) Hirsch (2009); (13) Copperwheat et al. (2011); (14) this paper.

luminosity classes I–V to be significantly different from those given for "normal" stars by Drilling and Landolt (1999), even though the stars in the present paper probably have much lower masses and luminosities.

5. Comparison with other systems

In Fig. 16, we compare the Green et al. (1986) classifications with the system that we have just defined. It is seen that the Green et al. classes sdOC, sdOB, and sdOD isolate He-strong stars of progressively later spectral class, from early O for class sdOC to early B for class sdOD, although there is a great deal of overlap in spectral class between these three Green et al. classes. Both C-strong and C-weak spectra are included in each of the three classes. The Green et al. classes sdB, sdB-O, sdOA, and sdOD isolate early B-type stars of progressively higher helium class, from a median of He3 for class sdB to He37 for sdOD, but again there is a large scatter in both spectral class and helium

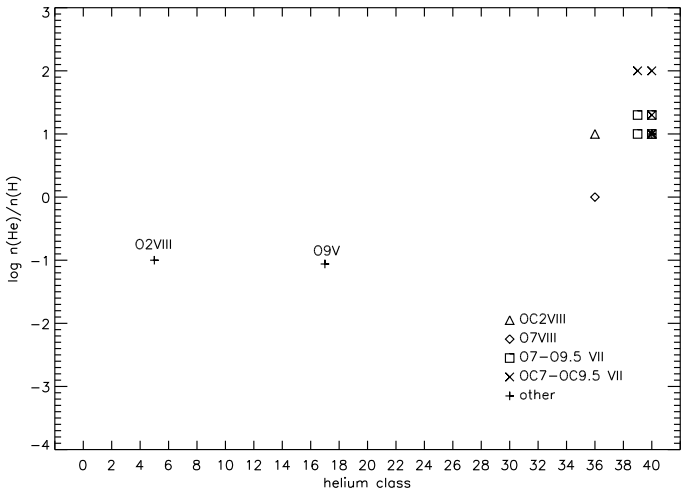

Fig. 13. Helium to hydrogen abundance ratio (by numbers of atoms) versus helium class for sdO stars.

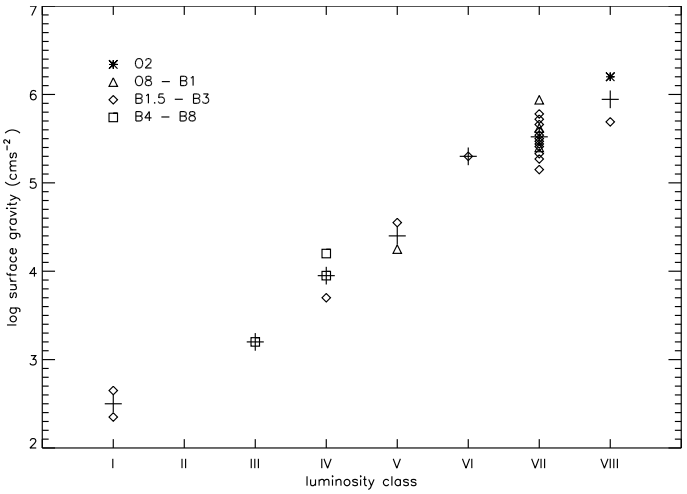

Fig. 14. Surface gravity versus luminosity class for helium class 0–18. The large crosses are the averages given in Table 4.

Table 4. Surface gravity calibration for helium class 0–18.

Luminosity class	$\log g$ [cm s^{-2}]	σ [cm s^{-2}]	n
I	2.50	±0.21	2
III	3.20	–	1
IV	3.95	±0.25	3
V	4.40	±0.21	2
VI	5.30	–	1
VII	5.52	±0.21	15
VIII	5.95	±0.36	2

class, and a lot of overlap in helium class, as would be expected from the much lower resolution spectra on which the Green et al. classes are based. The other Green et al. class represented here, HBB, tends to isolate late B-type stars of luminosity class III–V, but there is seen to be some overlap in Fig. 16 between the earlier HBB stars and the Green et al. types sdB and sdB-O. One sees from these figures that despite statements which have been made to the contrary (Jeffery et al. 1997), the Green et al. classes do define "natural" groups in the spectral class – helium class – luminosity class space defined by this paper.

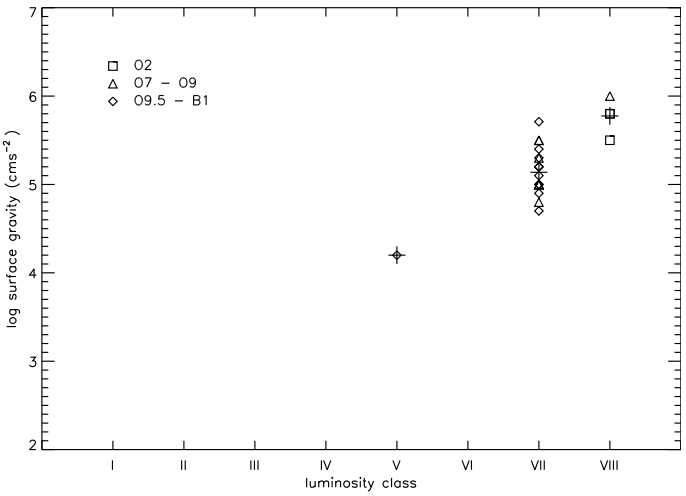

Fig. 15. Surface gravity versus luminosity class for helium class 24–40. The large crosses are the averages given in Table 5.

Table 5. Surface gravity calibration for helium class 24–40.

Luminosity class	$\log g$ [cm s^{-2}]	σ [cm s^{-2}]	n
V	4.20	–	1
VII	5.14	±0.26	19
VIII	5.78	±0.21	4

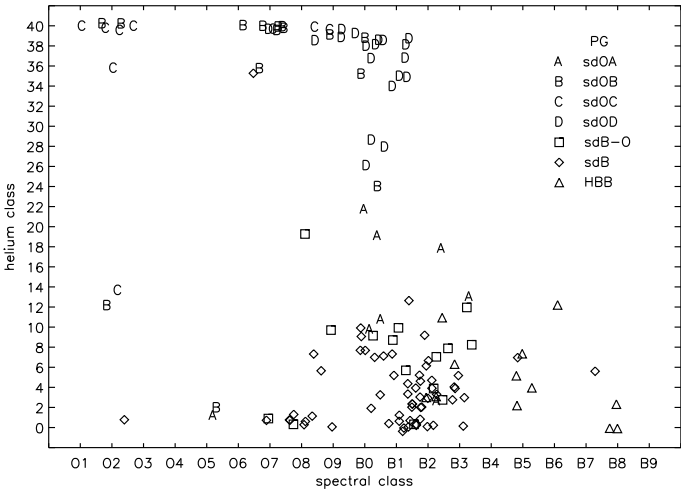

Fig. 16. Comparison of the new spectral and helium classes with the PG classes. The points have been given small random shifts to resolve overlap.

6. Conclusions

We have defined with standards an MK-like system for classifying hot subdwarfs which merges smoothly with the MK system itself in the following respects:

1. The spectral types of helium-normal stars have been defined such that all line ratios are roughly the same as they are for MK standards of the same spectral class (and luminosity class for luminosity classes I–V).
2. The spectral types of helium-strong stars have been defined such that all line ratios for different ions of the same element are roughly the same as they are for MK standards of the same spectral class.

3. The spectral types of helium-weak stars have been defined such that the Balmer-line widths and depths are roughly the same as they are for helium-normal stars of the same spectral type.
4. The spectra of the blue horizontal-branch stars and other stars which are not hot subdwarfs have essentially been classified using MK standards (except for the helium class).

We find that two parameters in addition to the MK-like spectral and luminosity classes are required to classify these stars: a helium class which depends on the relative strengths of the H and He lines, and a "C" designation to denote carbon-strong spectra. Preliminary calibrations of effective temperature versus spectral class, helium abundance versus helium class, and surface gravity versus luminosity class have been made, but much work remains to be done. Finally, spectra from a large number of surveys in progress remain to be classified, and this will doubtlessly cause the system to evolve.

Acknowledgements. We gratefully acknowledge the ESO and Calar Alto Observatories. This research made use of the SIMBAD database, operated at CDS, Strasbourg, France, and was supported in part by National Science Foundation grant AST-9819835. We thank Chris Copperwheat for providing us with his spectra of PG1432+004, PG1644+404 and PG2314+076. We especially wish to thank the referee, N.R. Walborn, whose many comments and suggestions greatly improved both the science and the readability of the paper.

References

Ahmad, A., & Jeffery, C. S. 2003, A&A, 402, 335
Bidelman, W. P. 1952, ApJ, 116, 227
Conlon, E. S., Theissen, A., & Moehler, S. 1993, A&A, 269, L1
Copperwheat, C. M., Morales-Rueda, L., Marsh, T. R., Maxted, P. F. L., & Heber, U. 2011, MNRAS, 415, 1381
Dreizler, S., Heber, U., Werner, K., Moehler, S., & de Boer, K. S. 1990, A&A, 235, 234
Drilling, J. S. 1996, in Hydrogen-Deficient Stars, eds. C. S. Jeffery, & U. Heber (San Francisco: ASP), 461
Drilling, J. S., & Landolt, A. U. 1999, in Allen's Astrophysical Quantities, ed. A. N. Cox (New York: Springer Verlag), 381
Green, R. F., Schmidt, M., & Liebert, J. 1986, ApJS, 61, 305
Hirsch, H. A. 2009, Ph.D. Thesis, Universität Erlangen-Nürnberg
Jeffery, C. S., Drilling, J. S., Harrison, P. M., Heber, U., & Moehler, S. 1997, A&AS, 125, 501
Keenan, P. C. 1987, PASP, 99, 713
Lester, J. B., Gray, R. O., & Kurucz, R. L. 1986, ApJS, 61, 509
Maxted, P. F. L., Heber, U., Marsh, T. R., & North, R. C. 2001, MNRAS, 326, 1391
Moehler, S., & Heber, U. 1998, A&A, 335, 985
Moehler, S., Richtler, T., de Boer, K. S., Dettmar, R. J., & Heber, U. 1990a, A&AS, 86, 53
Moehler, S., Heber, U., & de Boer, K. S. 1990b, A&A, 239, 265
Moehler, S., Heber, U., & Dreizler, S. 1994, A&A, 282, L29
Morales-Rueda, L., Maxted, P. F. L., Marsh, T. R., North, R. C., & Heber, U. 2003, MNRAS, 338, 752
Morgan, W. W. 1984, in The MK Process and Stellar Classification, ed. R. F. Garrison (Toronto: David Dunlap Obs.), 18
Morgan, W. W., Keenan, P. C., & Kellman, E. 1943, An Atlas of Stellar Spectra (Chicago: University of Chicago Press)
Napiwotzki, R. 1993, Acta Astron., 43, 343
Napiwotzki, R., Schönberner, D., & Wenske, V. 1993, A&A, 268, 653
Østensen, R. H. 2006, Baltic Astron., 15, 85
Ramspeck, M., Heber, U., & Edelmann, H. 2001, A&A, 379, 235
Saffer, R. A., Bergeron, P., Koester, D., & Liebert, J. 1994, ApJ, 432, 351
Salomon, Z. 2003, Diploma thesis, Universität Erlangen-Nürnberg
Schmidt, J. H. K. 1996, Ph.D. Thesis, Universität Bonn
Sota, A., Maiz Apellániz, J., Walborn, N. R., et al. 2011, ApJS, 193, 24
Theissen, A., Moehler, S., Heber, U., & de Boer, K. S. 1993, A&A, 273, 524
Theissen, A., Moehler, S., Heber, U., Schmidt, J. H. K., & de Boer, K. S. 1995, A&A, 298, 577
Walborn, N. R. 1971 ApJS, 23, 257
Walborn, N. R. 1976, ApJ, 205, 419
Walborn, N. R., & Fitzpatrick, E. L. 1990, PASP, 102, 379
Walborn, N. R., Howarth, I. D., Lennon, D. J., et al. 2002, AJ, 123, 2754
Walborn, N. R., Sota, A., Maiz Apellániz, J., et al. 2010, ApJ, 711, L143
Winter, C., Jeffery, C. S., & Drilling, J. S. 2004, Astrophys. Space Sci., 291, 375
Winter, C., Jeffery, C. S., Ahmad, A., & Morgan, D. R. 2006, Baltic Astron., 15, 69